Scaling of nodal resilience and influence in complex dynamical networks

Li-Lei Han,[1] Lang Zeng,[1] Hayoung Choi,[1] Ying-Cheng Lai,[2,3] and Younghae Do[1,a)]
[1)] *Department of Mathematics, Nonlinear Dynamics & Mathematical Application Center, Kyungpook National University, Daegu, 41566, Republic of Korea*
[2)] *School of Electrical, Computer and Energy Engineering, Arizona State University, Tempe, 85287, USA*
[3)] *Department of Physics, Arizona State University, Tempe, 85287, USA*

(Dated: 9 January 2025)

In complex dynamical networks, the resilience of the individual nodes against perturbation and their influence on the network dynamics are of great interest and have been actively investigated. We consider situations where the coupling dynamics are separable, which arise in certain classes of dynamical processes including epidemic spreading, population dynamics, and regulatory processes, and derive the algebraic scaling relations characterizing the nodal resilience and influence. Utilizing synthetic and empirical networks of different topologies, we numerically verify the scaling associated with the dynamical processes. Our results provide insights into the interplay between network topology and dynamics for the class of processes with separable coupling functions.

In applications involving complex dynamical networks, it is often of interest to assess the ability of individual nodes to withstand disruptions or perturbations. This defines the nodal resilience. A network with more resilient nodes is naturally more resistant to global catastrophic dynamical events such as cascading failures. It is also useful to quantify an individual node's influence on the behaviors of other nodes in the network, as such influences determine the dynamics on the whole network. Are there general scaling relations characterizing the dependence of nodal resilience and influence on the degree? To answer this question for arbitrary nodal dynamical interactions is difficult. However, if the node-to-node coupling dynamics are separable, the scaling relations exist and can be derived analytically. Situations where complex networks host separable coupling dynamics can in fact arise in physical and biological contexts such as epidemic spreading, population dynamics, and regulatory processes. This article presents an analytic theory to show that both nodal resilience and influence scale with the degree algebraically, with extensive numerical support from a large number of synthetic and empirical networks of different topologies. The algebraic scaling relations are robust against variations in network properties such as the clustering coefficient, degree correlation and heterogeneity. The findings provide insights into the interplay between network topology and dynamics for tasks such as robustness analysis, critical node identification, and network stability enhancement.

I. INTRODUCTION

Extensive research has established that the structures of many complex networks in the real world, to some extent, exhibit general features including random[1], small-world[2], and scale-free[3,4] topologies. In addition to these three well studied topologies, networks possessing a self-similar structure can also arise[5]. Each topology can be generated by a set of elementary governing rules, e.g., the preferential-attachment rule that results in the scale-free topology[3,4]. Complex networks in the real world host dynamical processes, leading to complex dynamical networked systems. Well studied processes include epidemic transmission[6–9], traffic flows[10], biological competitions[11–13], cascading failures[14–16], and cellular signaling[17–23].

Considerable efforts were devoted to searching for general dynamical behaviors on complex networks. Earlier, a class of dynamics on weighted complex networks was uncovered[24], where the topological details of various properly weighted real-world networks tend to have little influence on a variety of dynamical processes on the network, suggesting the possibility of developing general strategies for controlling network dynamics. The networks can be biological, physical, technological, or social, and the dynamical processes studied include synchronization, epidemic spreading, and percolation. Later, some common network dynamics were identified[25] and it was also found that a diverse array of flow patterns on complex networks can be mapped into and described by some specific function[26,27]. Subsequently, three generic modes associated with spatiotemporal signal propagation in complex networks were discovered: distance-limited, degree-limited, and composite propagation[28]. Quite recently, discrete stability categories in complex networked dynamics were unveiled: asymptotically unstable, sensitive, and asymptotically stable[29].

In this paper, we investigate nodal resilience and influence in complex dynamical networks. In particu-

[a)] Electronic mail: yhdo@knu.ac.kr

lar, an individual node's resilience measures its capability to withstand disruptions or perturbations, which underscores the robustness of the entire system[30]. A node's influence on the network dynamics is also of interest, as certain nodes can have a disproportional effect on the interactions and information flow in the network[31,32]. Studies also offered insights into the related issue of adaptive mechanisms of nodes in dynamical networks[30,33,34] and the evolving landscape of nodal influences[35,36]. In spite of these works, a theoretical framework to explain the resilience and influence of nodes was lacking. To partially address this issue, we consider a special class of dynamical networks whose coupling dynamics are separable and investigate the scaling of the resilience and influence with the nodal degree under short-term or long-term perturbations. Representative dynamical processes with separable coupling functions include certain classes of epidemic spreading, population dynamics, and regulatory processes. We analytically find that the scaling is algebraic and validate them using synthetic and empirical networks. Depending on the specific dynamical process, the nodal resilience and influence can be degree enhancing, degree uniform, or degree suppressing. Our results offer further insights into the interplay between network topology and dynamics for tasks such as robustness analysis, critical node identification, and network stability enhancement.

II. NODAL RESILIENCE AND INFLUENCE

We consider a complex dynamical network comprising N interconnected nodes represented by a weighted, undirected adjacency matrix A_{ij}. The system dynamics are governed by

$$\frac{dx_i}{dt} = M_0(x_i) + \sum_{j=1}^{N} A_{ij} M_1(x_i) M_2(x_j), \tag{1}$$

where $x_i(t)$ is the vector of the dynamical variables of node i, $M_0(x_i(t))$ characterizes the self-evolution of node i, the product of the functions $M_1(x_i(t))$ and $M_2(x_j(t))$ describes the pairwise interaction between nodes i and j, so the coupling is separable. In spite of this separability assumption, Eq. (1) can model certain dynamical processes such as epidemics (denoted as **E**)[6–9], population dynamics (denoted as **P**)[37], and regulatory dynamics (denoted as **R**)[17,19,20,22,23]. Consider the situation where the system has attained a steady state when a disturbance occurs, with nodal values stabilized at x_i. Introducing a small temporary perturbation δx_m at node m, we reset the time to 0. The initial conditions for the nodes in the network are thus given by

$$x_i(0) = \begin{cases} x_i, & i \neq m, \\ x_m + \delta x_m, & i = m. \end{cases} \tag{2}$$

A. Steady-state solution

The steady state of the networked dynamical system Eq. (1) can be obtained by solving

$$\frac{dx_i}{dt} = M_0(x_i) + \sum_{j=1}^{N} A_{ij} M_1(x_i) M_2(x_j) = 0. \tag{3}$$

The average of $M_2(x_j)$ among neighboring nodes is

$$\langle M_2(x) \rangle_i = \frac{1}{k_i} \sum A_{ij} M_2(x_j), \tag{4}$$

where k_i denotes the degree of node i. Substituting Eq. (4) into Eq. (3), we have

$$M_0(x_i) + k_i M_1(x_i) \langle M_2(x) \rangle_i = 0. \tag{5}$$

Letting

$$R(x_i) \equiv -\frac{M_1(x_i)}{M_0(x_i)}, \tag{6}$$

we have, from Eq. (5),

$$R(x_i) = \frac{1}{k_i \langle M_2(x) \rangle_i}. \tag{7}$$

For $\lambda_i \equiv R(x_i)$, we have $\lambda_i \sim k_i^{-1}$, so the steady state x_i can be obtained through the inverse of $R(x_i)$:

$$x_i = R^{-1}(\lambda_i). \tag{8}$$

B. Definition of nodal resilience and influence

After a temporary perturbation, the system undergoes a transient phase before returning to its steady state. The instantaneous response of node m is

$$\Delta x_m(t) = x_m(t) - x_m, \tag{9}$$

where $\Delta x_m(t)$ measures the deviation of node m from its steady state. To quantify the resilience of node m, we use the concept of resilience triangle[38]. The loss of resilience of node m is defined as

$$\mathrm{LR}_m = \int \frac{\Delta x_m(t)}{\delta x_m} dt, \tag{10}$$

where the integrand $\Delta x_m(t)/\delta x_m$ is positive[38], so $\mathrm{LR}_m > 0$. A larger value of LR_m means that it takes longer for the node to recover to its steady state, signifying a weaker resilience. The resilience R_m of node m can then be defined as the reciprocal of LR_m, i.e.,

$$R_m = \frac{1}{\mathrm{LR}_m}. \tag{11}$$

A smaller resilience loss LR_m corresponds to a higher resilience R_m, meaning that the node is more capable of returning to its steady state.

The influence I_m of node m on the rest of the network is defined as the cumulative resilience losses of other nodes in the system:

$$I_m = \sum_{i=1, i\neq m}^{N} \mathrm{LR}_i = \sum_{i=1, i\neq m}^{N} \int \frac{\Delta x_i(t)}{\delta x_m} dt, \tag{12}$$

where larger resilience losses of the other nodes indicate that the influence of node m is greater.

III. SCALING OF NODAL RESILIENCE

A perturbation δx_m applied to the steady state of node m gives the initial condition: $x_m(0) = x_m + \delta x_m$, e.g., $\delta x_m = \alpha x_m$ with $\alpha = 0.1$. The dynamical evolution of m is governed by

$$\frac{d(x_m + \Delta x_m(t))}{dt} = M_0(x_m + \Delta x_m(t)) + \sum_{j=1}^{N} A_{mj} M_1(x_m + \Delta x_m(t)) M_2(x_j + \Delta x_j(t)), \tag{13}$$

where $\Delta x_m(t)$ is the instantaneous response of node m, as defined in Eq. (9). Linearizing the dynamics about the steady state, we obtain

$$\frac{d\Delta x_m(t)}{dt} = \left(M_0'(x_m) + M_1'(x_m) \sum_{j=1}^{N} A_{mj} M_2(x_j) \right) \Delta x_m(t) + M_1(x_m) \sum_{j=1}^{N} A_{mj} M_2'(x_j) \Delta x_j(t) + o(\Delta x^2). \tag{14}$$

For $\Delta x_j(t) \ll \Delta x_m(t)$, Eq. (14) can be simplified as

$$\frac{d\Delta x_m(t)}{dt} = P_m \Delta x_m(t), \tag{15}$$

where

$$P_m = M_0'(x_m) + M_1'(x_m) \sum_{j=1}^{N} A_{mj} M_2(x_j).$$

Solving Eq. (15), we get

$$\Delta x_m(t) = \delta x_m e^{P_m t}. \tag{16}$$

Consequently, the resilience of node m can be obtained as

$$R_m = \frac{1}{\int \frac{\Delta x_m(t)}{\delta x_m} dt} = -P_m. \tag{17}$$

Employing Eq. (6), we have

$$M_0'(x_m) = -\frac{M_1'(x_m)}{R(x_m)} + \frac{M_1(x_m) R'(x_m)}{R^2(x_m)}. \tag{18}$$

Utilizing Eqs. (4) and (7), we get

$$M_1'(x_m) \sum_{j=1}^{N} A_{mj} M_2(x_j) = \frac{M_1'(x_m)}{R(x_m)}. \tag{19}$$

Combining these expressions, we finally obtain

$$P_m = \frac{M_1(x_m) R'(x_m)}{\lambda_m^2}. \tag{20}$$

Using the Hahn series, $M_1(x_m)$ and $R'(x_i)$ can be expressed as

$$M_1(x_m) = \sum_{n=0}^{\infty} B_n \lambda_m^{\beta_n} \quad \text{and} \quad R'(x_m) = \sum_{n=0}^{\infty} C_n \lambda_m^{\psi_n}. \tag{21}$$

In the limit $\lambda_m \to 0$, the leading terms $\lambda_m^{\beta_0}$ and $\lambda_m^{\psi_0}$ dominate the dynamical evolution. We have

$$R_m \sim \lambda_m^{-2+\beta_0+\psi_0}. \tag{22}$$

Utilizing $\lambda_m \sim k_m^{-1}$, we also have

$$R_m \sim k_m^{2-\beta_0-\psi_0}, \tag{23}$$

where

$$\zeta = 2 - \beta_0 - \psi_0. \tag{24}$$

It can be seen from Eqs. (23) and (24) that the nodal resilience scales with the nodal degree algebraically with the exponent ζ.

To provide numerical support for the scaling relations (23) and (24), we implement epidemic spreading (**E**),

population dynamics (**P**), and regulatory dynamics (**R**) on ER (Erdös-Rényi) random and scale-free networks. The details of the network structures and dynamical processes are listed in Tab. I. The expressions of the scaling exponents for the **E**, **R**, and **P** dynamics are provided in Appendix A.

TABLE I. Network dynamics

Dynamics	Equation	Notation
Epidemic	$\frac{dx_i}{dt} = -x_i(t) + \sum_{j=1}^{N} A_{ij}\,(1 - x_i(t))\,x_j(t)$	**E**
Population	$\frac{dx_i}{dt} = -x_i^{0.8}(t) + \sum_{j=1}^{N} A_{ij} x_j^{0.2}(t)$	**P**
Regulatory	$\frac{dx_i}{dt} = -x_i(t) + \sum_{j=1}^{N} A_{ij} \frac{x_j(t)}{1+x_j(t)}$	**R**

Under an impulsive perturbation, the scaling of the nodal resilience with the degree exhibits three distinct behaviors, as shown in Figs. 1(a), 1(b), and 1(c), respectively, for **E**, **R**, and **P** types of dynamics. For $\zeta > 0$, the nodal resilience increases with the degree, indicating that the hub nodes are more resilient. For $\zeta \approx 0$, the nodes in the network are uniformly resilient against the perturbation. For $\zeta < 0$, nodes of smaller degrees tend to be more resilient.

IV. SCALING OF NODAL INFLUENCE I_m

We first consider the case where the perturbation is impulsive and applies to node m at $t = 0$. The dynamics of the nearest neighbor of node m, denoted as i, described by the following equation:

$$\frac{d(x_i + \Delta x_i(t))}{dt} = M_0(x_i + \Delta x_i(t)) + \sum_{j=1}^{N} A_{ij} M_1(x_i + \Delta x_i(t)) M_2(x_j + \Delta x_j(t)), \tag{25}$$

which can be linearized about the steady state as

$$\begin{aligned}\frac{d\Delta x_i(t)}{dt} = &\left(M_0'(x_i) + M_1'(x_i) \sum_{j=1}^{N} A_{ij} M_2(x_j) \right) \Delta x_i(t) \\ &+ M_1(x_i) \sum_{j=1, j\neq m}^{N} A_{ij} M_2'(x_j) \Delta x_j(t) \\ &+ M_1(x_i) M_2'(x_m) \Delta x_m(t) + o(\Delta x^2).\end{aligned} \tag{26}$$

Assuming that node j is far from the disturbance source m, we have $\Delta x_j(t) \ll \Delta x_m(t)$. Equation (26) can then be written as

$$\frac{d\Delta x_i(t)}{dt} = P_i \Delta x_i(t) + Q_i, \tag{27}$$

where

$$\begin{aligned}P_i &= M_0'(x_i) + M_1'(x_i) \sum_{j=1}^{N} A_{ij} M_2(x_j) \text{ and} \\ Q_i &= M_1(x_i) M_2'(x_m) \Delta x_m(t).\end{aligned}$$

Solving Eq. (27) gives

$$\Delta x_i(t) = e^{P_i t} \int Q_i e^{\int -P_i dt} dt. \tag{28}$$

Substituting Eq. (16) into Eq. (28), we get

$$\Delta x_i(t) = \frac{M_1(x_i) M_2'(x_m) \delta x_m}{P_m - P_i} (e^{P_m t} - e^{P_i t}). \tag{29}$$

Consequently, the loss of resilience of node i can be obtained as

$$LR_i = \int \frac{\Delta x_i(t)}{\delta x_m} dt = \frac{M_1(x_i) M_2'(x_m)}{P_i P_m}. \tag{30}$$

Similarly, $M_2'(x_m)$ can be expressed as a Hahn series:

$$M_2'(x_m) = \sum_{n=0}^{\infty} C_n \lambda_m^{\varphi_n}, \tag{31}$$

which can be simplified as

$$M_2'(x_m) \sim k_m^{-\varphi_0}. \tag{32}$$

Combining Eqs. (17), (23) and (30), we get

$$LR_i \sim k_m^{-2+\beta_0+\psi_0-\varphi_0}. \tag{33}$$

Collecting all neighboring nodes of the perturbed node m, we obtain the scaling relation:

$$I_m \sim k_m^{\eta}, \tag{34}$$

with the algebraic scaling exponent η given by

$$\eta = -1 + \beta_0 + \psi_0 - \varphi_0. \tag{35}$$

We next consider a constant perturbation: $\Delta x_m(t) = \delta x_m$. In this case, the nodal resilience cannot be defined, but the influence Z_m of node m can be defined as

$$Z_m = \sum_{i=1, i\neq m}^{N} \frac{\Delta x_i(t \to \infty)}{\delta x_m}, \tag{36}$$

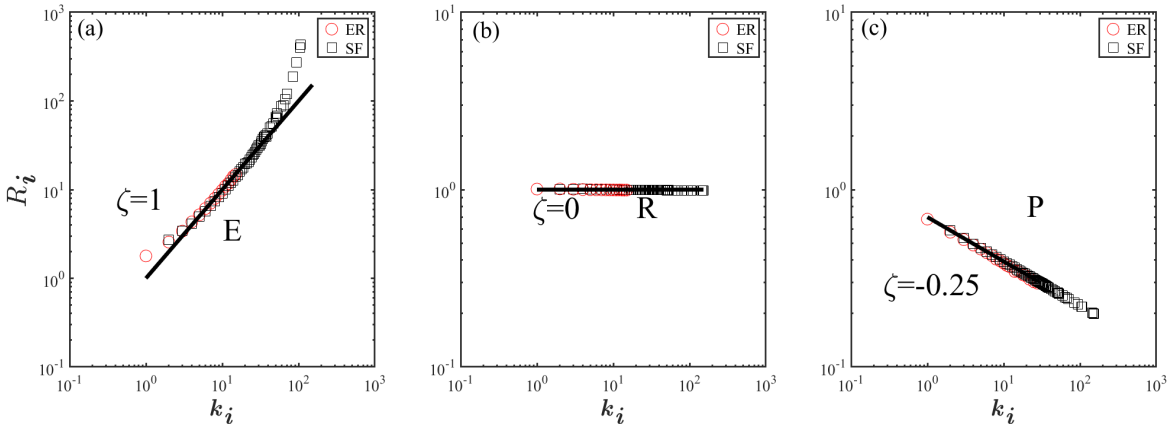

FIG. 1. Patterns of nodal resilience under temporary perturbation. (a-c) R_i versus k_i for **E**, **R**, and **P**, respectively, for all networks. The red circles represent the results from an Erdős-Rényi random network with size $N = 6,000$ and average degree $\langle k\rangle = 4$, and the black diamonds give the results from a scale-free network of size $N = 6,000$ and average degree $\langle k\rangle = 4$.

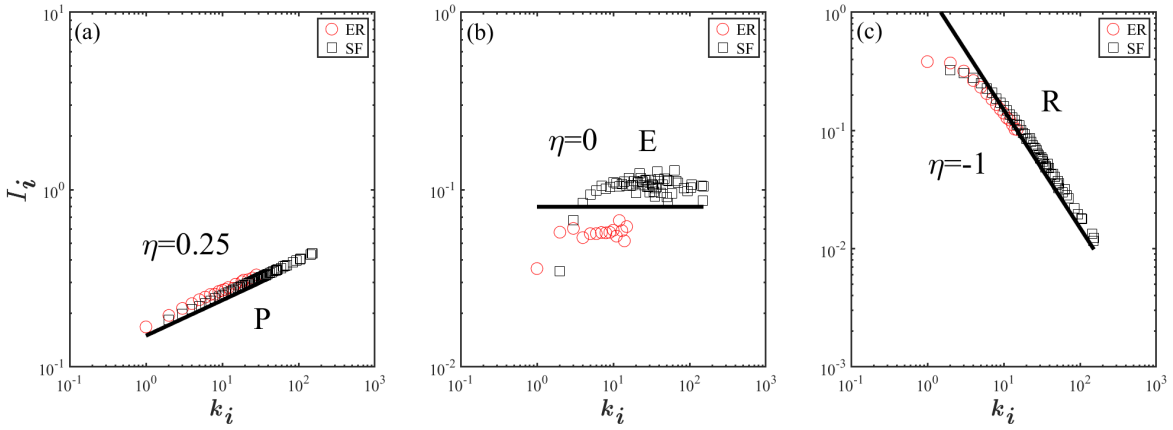

FIG. 2. Patterns of nodal influence under temporary perturbation. (a-c) I_i versus k_i for **P**,**E**, and **R**, respectively, for all networks. The red circles represent the results from an Erdős-Rényi random network with size $N = 6,000$ and average degree $\langle k\rangle = 4$, and the black diamonds give the results from a scale-free network of size $N = 6,000$ and average degree $\langle k\rangle = 4$.

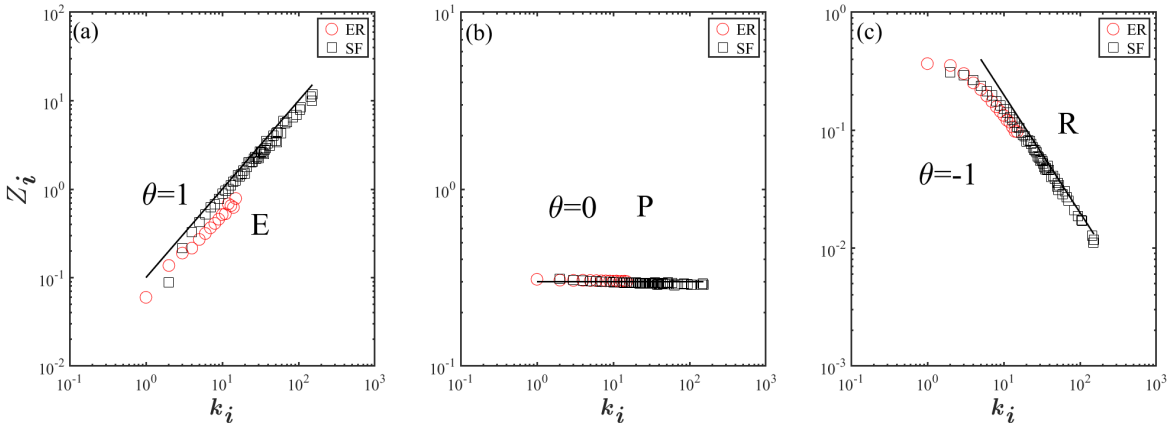

FIG. 3. Patterns of nodal influence under a constant perturbation. (a-c) Z_i versus k_i for **E**,**P**, and **R**, respectively, for all networks. The red circles represent the results from an Erdős-Rényi random network with size $N = 6,000$ and average degree $\langle k\rangle = 4$, and the black diamonds give the results from a scale-free network of size $N = 6,000$ and average degree $\langle k\rangle = 4$.

where $\Delta x_i(t \to \infty)$ is the ith node's response to the disturbance at the source m. From Eq. (27), we get

$Q_i = M_1(x_i)M_2'(x_m)\delta x_m$. From Eq. (28), we obtain

$$\Delta x_i(t) = \frac{M_1(x_i)M_2'(x_m)\delta x_m}{P_i}(e^{P_i t} - 1). \tag{37}$$

In the limit $t \to \infty$, we get

$$\frac{\Delta x_i(t \to \infty)}{\delta x_m} = -\frac{M_1(x_i)M_2'(x_m)}{P_i} \sim k_m^{-\varphi_0}, \tag{38}$$

and the scaling relation:

$$Z_m \sim k_m^{\theta}, \tag{39}$$

where

$$\theta = 1 - \varphi_0. \tag{40}$$

To verify the scaling relations (34) and (35) for the case of an impulsive perturbation, we use the same numerical setting as in Fig. 1. The results are shown in Fig. 2. It can be seen that the nodal influence also exhibits three distinct scaling behaviors, as shown in Figs. 2(a), 2(b), and 2(c) for **P**, **E**, and **R** types of dynamics, respectively. For the case of a constant perturbation, the simulation results to support the scaling relations as given by (39) and (40) are shown in Fig. 3. There are again three distinct patterns: (1) for **E** type of dynamics, we have $\theta = 1$, indicating that nodes with larger degrees have greater influence on other nodes, (2) for **P** type of dynamics, we have $\theta \approx 0$, so the nodal influence is independent of the degree, and (3) for **R** type of dynamics, we have $\theta = -1$. In this case, nodes with smaller degrees have greater influence.

V. VERIFYING RESILIENCE AND INFLUENCE SCALING WITH EMPIRICAL NETWORKS

We study the following empirical networks to test the scaling:

1. **PPI1** The yeast scale-free protein-protein interaction network, consisting of 1,647 nodes (proteins) and 5,036 undirected links. The network describes the chemical interactions among proteins[39].
2. **PPI2** The human protein-protein interaction network, a scale-free network, consisting of N = 2,035 nodes (protein) and L = 13,806 protein-protein interaction links[40].
3. **PPI3** Binary protein-protein interaction network of Arabidopsis thaliana, whose giant connected component comprises 2,938 nodes and 7,720 links[41].
4. **PPI4** Multiplex genetic and protein interactions network of Rattus norvegicus, composed of 2,350 nodes and 3,484 links[42].
5. **URIV** The email communication network at the University Rovira i Virgili in Tarragona in the south of Catalonia in Spain, composed of 1,133 nodes and 5,451 links[43].
6. **UCIonline** An instant messaging network from the University of California Irvine[44], capturing 61,040 transactions between 1,893 users during a 218-day period. Connecting all individuals who exchanged messages throughout the period leads to a network of 1,893 nodes with 27,670 links, exhibiting a fat-tailed degree distribution.
7. **ECO1** A mutualistic ecological network constructed using data on symbiotic interactions of plants and pollinators in Carlinville, Illinois[28]. The resulting network is a bipartite graph linking 456 plants with 1,429 pollinators. When a pair of plants is visited by the same pollinator, they mutually benefit each other indirectly by increasing the pollinator populations. Similarly, pollinators sharing the same plants possess an indirect mutualistic interaction.

TABLE II. Structural characteristics of the empirical networks, including the number N of nodes, the average degree $\langle k \rangle$, assortativity coefficient r, and clustering coefficient C. The rightmost column indicates the dynamical processes implemented in the simulations.

Network	N	$\langle k \rangle$	r	C	Dynamics
PPI1	1647	3.05	-0.1059	0.1908	**R**
PPI2	2035	6.78	-0.2192	0.0473	**R**
PPI3	2938	5.25	-0.1929	0.1256	**R**
PPI4	2350	2.96	-0.1856	0.0853	**R**
URIV	1133	9.62	0.0782	0.1662	**E**
UCIonline	1893	14.61	-0.1880	0.1097	**E**
ECO1	1044	14.17	-0.1740	0.0376	**P**

Table II lists the structural characteristics of the empirical networks and the corresponding dynamical processes. Simulations reveal the three distinct scaling behaviors governing the nodal resilience and influence as predicted by theory, as shown in Figs. 4, 5, and 6.

VI. DISCUSSION

We have studied the degree scaling of nodal resilience and influence for a class of complex dynamical networks that satisfy the separability condition: the coupling between a pair of nodes can be written as the product of two functions, each depending solely on the dynamical variable of the respective node. While this assumption may be strong so as to make an analytic derivation of the scaling relations possible, certain types of dynamical processes on networks do satisfy this assumption, which include epidemic spreading, population dynamics, and regulatory processes. Given a specific type of dynamical process on the network, e.g., epidemic spreading,

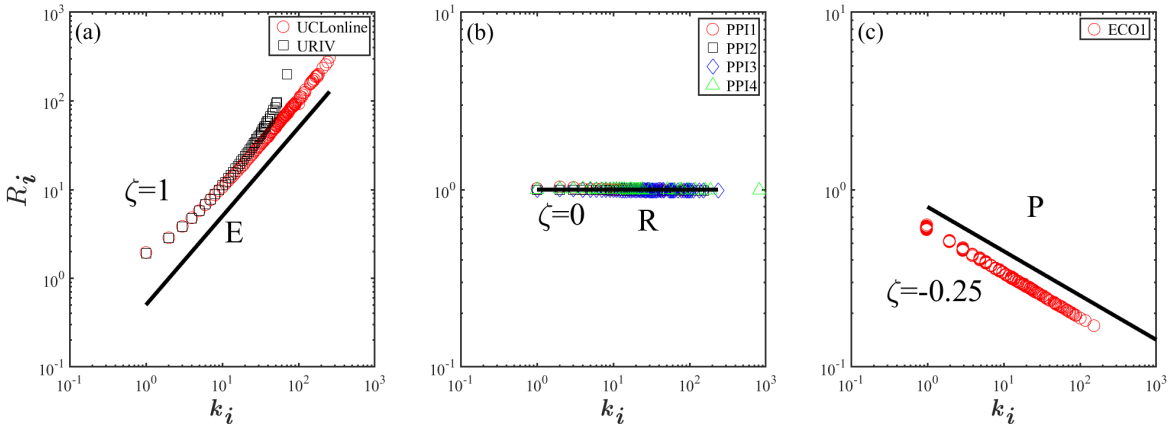

FIG. 4. Scaling of nodal resilience for empirical networks. Shown is R_i versus k_i for (a) **E** dynamics, (b) **R** dynamics, and (c) **P** dynamics.

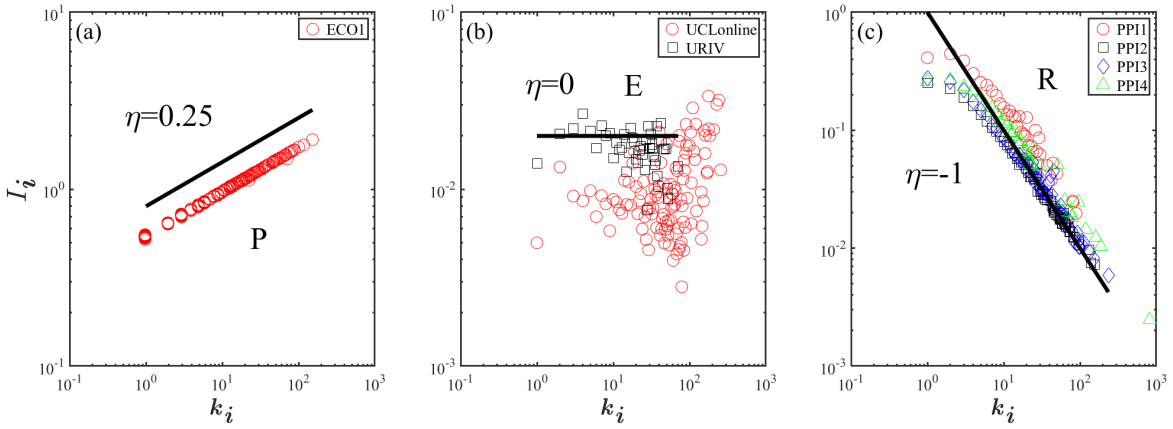

FIG. 5. Scaling of nodal influence under an impulsive perturbation. Shown is I_i versus k_i for (a) **P** dynamics, (b) **E** dynamics, and (c) **R** dynamics.

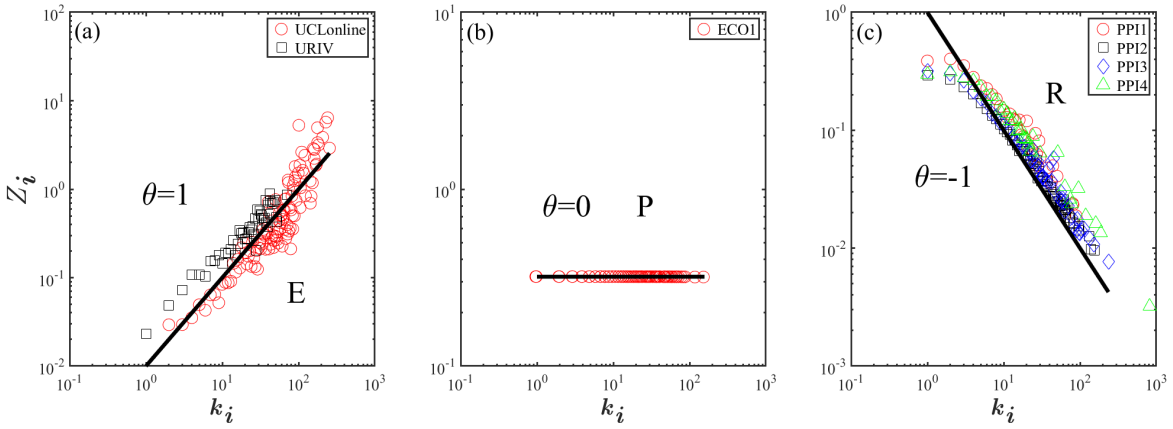

FIG. 6. Scaling of nodal influence under a constant perturbation. Shown is Z_i versus k_i for (a) **E** dynamics, (b) **P** dynamics, and (c) **R** dynamics.

the roles played by the individual nodes in the process, which depend on the nodal degree, are of interest, especially from the standpoint of control and mitigation. For example, if it is determined that a small set of nodes contribute disproportionally to the spreading, some optimal control strategy at the nodal level can be devised

to suppress (or promote) the dynamics. Our theoretical analysis and extensive numerical computations using a large number of synthetic and empirical networks revealed that, regardless of the network structure, for a given type of dynamical process, the scaling relations of the nodal resilience and influence with the degree is algebraic, which holds with respect to variations in network properties such as the clustering coefficient, degree correlation and degree heterogeneity, even when the perturbation is large (Appendix B).

It is worth emphasizing that our theoretical derivations of the algebraic scaling of the nodal resilience and influence rely on the network dynamics settling into a stable state in the absence of any perturbation. Whether similar scaling would arise in networks with oscillatory dynamics is an open question. Another direction to extend our study is search for nodal resilience and influence scaling in multilayer and multiplex complex networks that model real-world systems with interdependencies.

ACKNOWLEDGMENT

This work was supported by the National Research Foundation of Korea (NRF) grant funded by the Korean government (MSIT) (Nos. NRF-2022R1A5A1033624 & 2022R1A2C3011711). The work at Arizona State University was supported by the Air Force Office of Scientific Research through Grant No. FA9550-21-1-0438.

Appendix A: Three types of network dynamics

1. Epidemic spreading dynamics

From the epidemics model in Tab. I, the three functions in Eq. (1) are $M_0(x) = -Bx$, $M_1(x) = 1 - x$ and $M_2(x) = x$. We have

$$R(x) = \frac{1-x}{Bx} \quad , R'(x) = \frac{1}{B}x^{-2} \quad \text{and } R^{-1}(x) = \frac{1}{1+Bx}.$$

Their Hahn expansions are

$$\begin{aligned} M_1\left(R^{-1}(x)\right) &= \frac{Bx}{1+Bx} = Bx - B^2x^2 + B^3x^3 - \cdots, \\ R'\left(R^{-1}(x)\right) &= \frac{1}{B} + 2x + Bx^2, \\ M_2'\left(R^{-1}(x)\right) &= 1. \end{aligned}$$

From Eqs. (21), (23), (31), (34) and (39), we get

$$\beta_0 = 1 \quad , \quad \psi_0 = 0 \quad \text{and} \quad \varphi_0 = 0, \tag{A1}$$

and

$$\zeta = 1 \quad , \quad \eta = 0 \quad \text{and} \quad \theta = 1. \tag{A2}$$

2. Regulatory dynamics

From the regulatory dynamics model shown in Tab. I, we have $M_0(x) = -Bx^a$, $M_1(x) = 1$ and $M_2(x) = \frac{x^h}{1+x^h}$, and

$$R(x) = \frac{1}{Bx^a}, \; R'(x) = -\frac{a}{B}x^{-(a+1)}, \; R^{-1}(x) = B^{-\frac{1}{a}}x^{-\frac{1}{a}}.$$

Their Hahn expansions are

$$\begin{aligned} M_1\left(R^{-1}(x)\right) &= 1, \\ R'\left(R^{-1}(x)\right) &= -aB^{\frac{1}{a}}x^{\frac{a+1}{a}}, \\ M_2'\left(R^{-1}(x)\right) &= \frac{hB^{-\frac{h-1}{a}}x^{-\frac{h-1}{a}}}{(1+B^{-\frac{h}{a}}x^{-\frac{h}{a}})^2} = hB^{\frac{h+1}{a}}x^{\frac{h+1}{a}} + \cdots. \end{aligned}$$

Substituting these expansions into Eqs. (21), (23), (31), (34) and (39), we get

$$\beta_0 = 0 \quad , \quad \psi_0 = \frac{a+1}{a} \quad \text{and} \quad \varphi_0 = \frac{h+1}{a}, \tag{A3}$$

and

$$\zeta = \frac{a-1}{a} \quad , \quad \eta = -\frac{h}{a} \quad \text{and} \quad \theta = 1 - \frac{h+1}{a}. \tag{A4}$$

As an example, for $a = 1$ and $h = 1$, we have $\zeta = 0$, $\eta = -1$ and $\theta = -1$.

3. Population dynamics

From the population dynamics model in Tab. I, we have $M_0(x) = -Bx^a$, $M_1(x) = 1$, and $M_2(x) = x^h$, leading to

$$R(x) = \frac{1}{Bx^a}, \; R'(x) = -\frac{a}{B}x^{-(a+1)}, \; R^{-1}(x) = B^{-\frac{1}{a}}x^{-\frac{1}{a}}.$$

Their Hahn expansions are

$$\begin{aligned} M_1\left(R^{-1}(x)\right) &= 1, \\ R'\left(R^{-1}(x)\right) &= -aB^{\frac{1}{a}}x^{\frac{a+1}{a}}, \\ M_2'\left(R^{-1}(x)\right) &= h(B^{-\frac{1}{a}}x^{-\frac{1}{a}})^{h-1} = hB^{-\frac{h-1}{a}}x^{-\frac{h-1}{a}}. \end{aligned}$$

Substituting the expansions into Eqs. (21), (23), (31), (34) and (39), we get

$$\beta_0 = 0 \; , \; \psi_0 = \frac{a+1}{a} \quad \text{and} \quad \varphi_0 = -\frac{h-1}{a}, \tag{A5}$$

and

$$\zeta = \frac{a-1}{a} \quad , \quad \eta = \frac{h}{a} \quad \text{and} \quad \theta = 1 + \frac{h-1}{a}. \tag{A6}$$

As an example, for $a = 0.8$ and $h = 0.2$, we have $\zeta = -0.25$, $\eta = 0.25$, and $\theta = 0$.

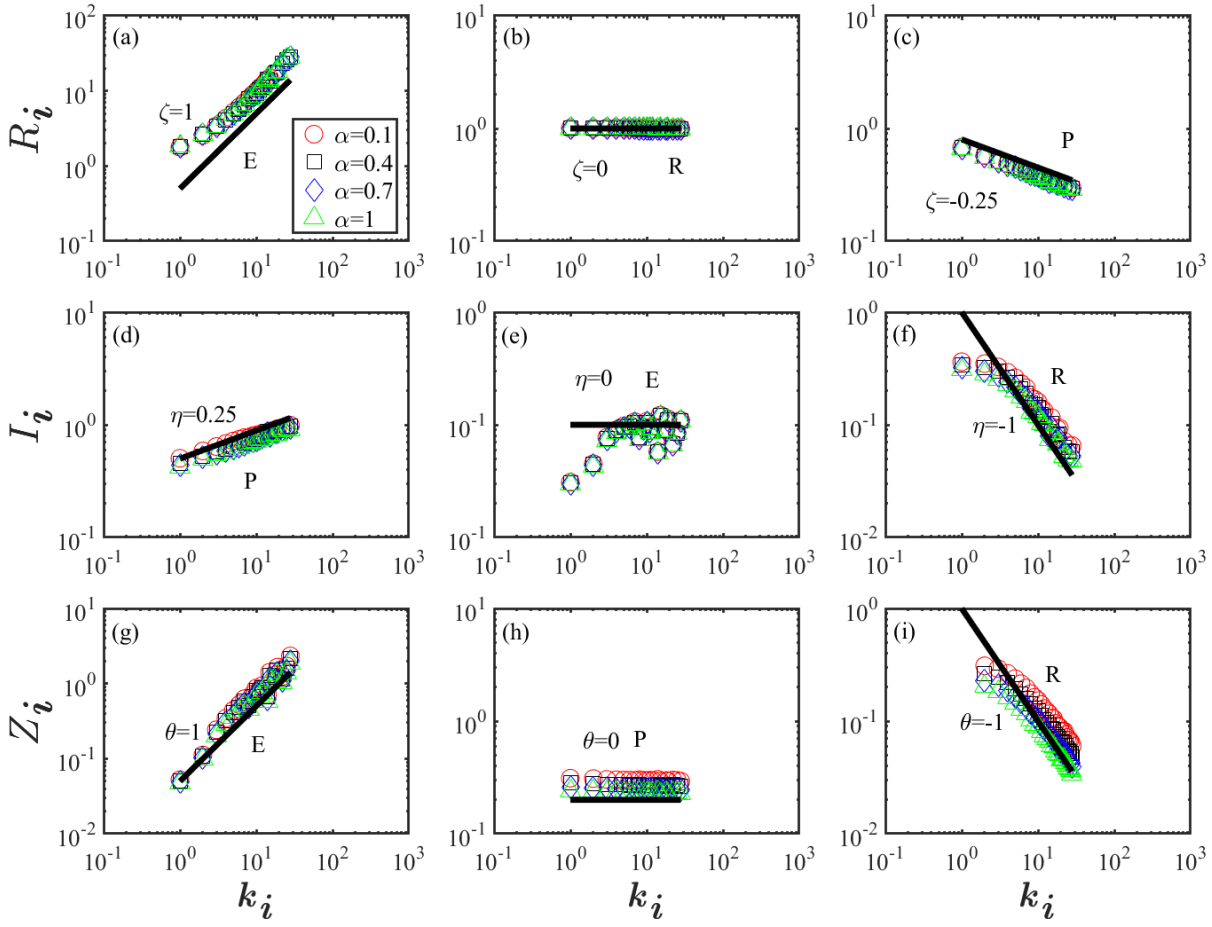

FIG. 7. Scaling of nodal resilience and influence with the degree under a large impulsive perturbation. The values of the relative perturbation magnitude are $\alpha = 0.4$, $\alpha = 0.7$ and $\alpha = 1$. (a-c) R_i versus k_i for **E**, **R**, and **P** types of dynamics, respectively. (d-f) I_i versus k_i for **P**, **E**, and **R** types of dynamics, respectively. (g-i) Z_i versus k_i for **E**, **P**, and **R** types of dynamics, respectively. The scaling is algebraic.

Appendix B: Effects of perturbation magnitude, network clustering coefficient, degree correlation and degree heterogeneity on scaling

1. Effect of perturbation magnitude

In our theoretical derivation of the nodal resilience and influence scaling, small perturbations are assumed: $\alpha = \Delta x_m/x_m \ll 1$, so that the approximation of linearized dynamics about the stable steady state is applicable. The simulation results in the main text are obtained with $\alpha = 0.1$. To find out if the three algebraic scaling relations hold for large perturbations, we set $\alpha = 0.4$, $\alpha = 0.7$ and $\alpha = 1$. The simulation results are shown in Fig. 7. It can be seen that, in spite of the large perturbation, the nodal resilience and influence still follow the three classes of algebraic scaling.

2. Effect of network clustering coefficient

The configuration model for complex networks stipulates that the clustering coefficient tends to zero if the network is sparse and large. However, empirical networks tend to have a nonzero clustering coefficient[45] (e.g., 0.1). To address the effects of the clustering coefficient C on the nodal resilience and influence scaling, we generate networks with $C = 0.15$ and calculate the scaling relations for different types of dynamical processes. The simulation results are shown in Fig. 8, revealing the emergence of the three classes of algebraic scaling.

3. Effect of degree correlation

We generate networks with three different values of the degree-degree correlation: $r = -0.2$, 0, and 0.2.

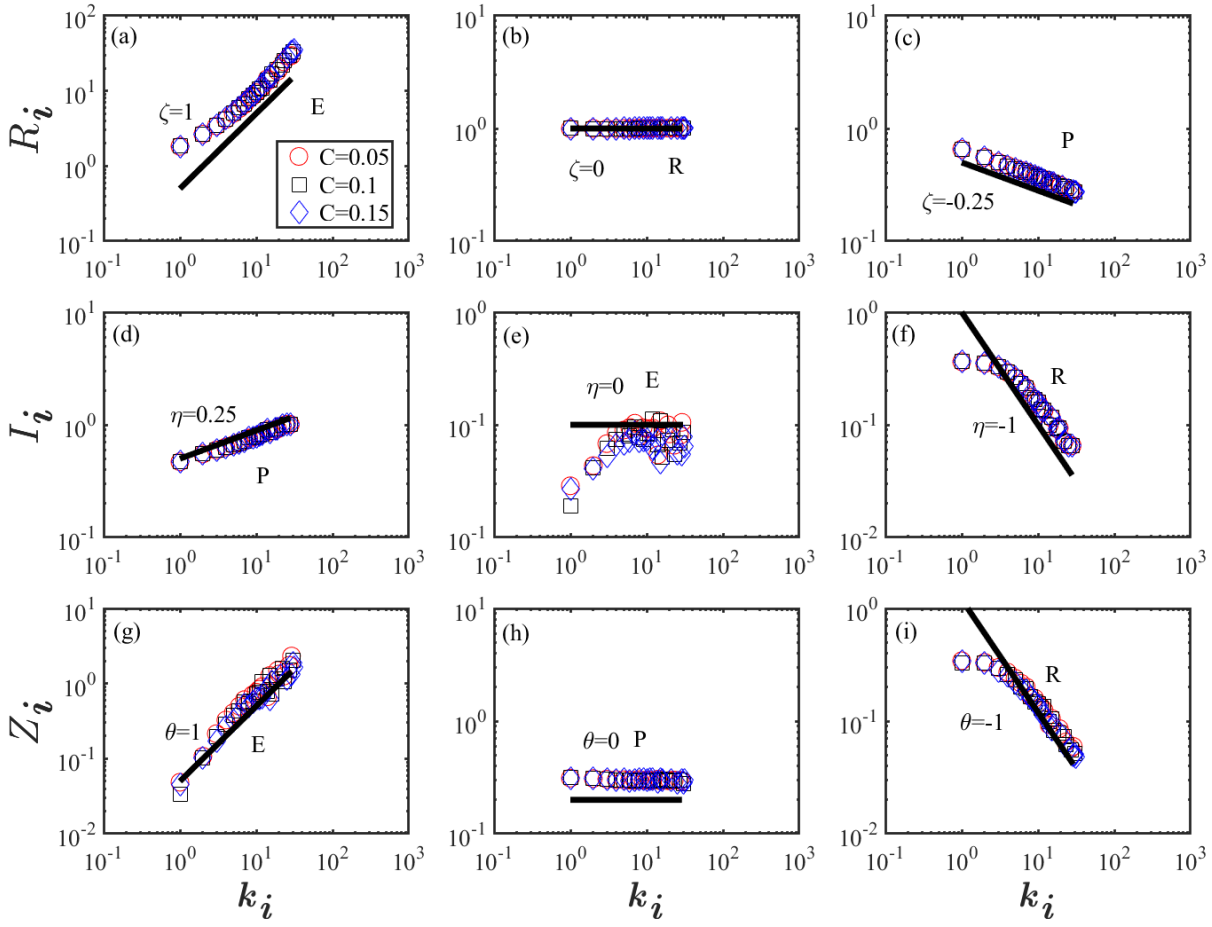

FIG. 8. Impact of network clustering coefficient on nodal resilience and influence scaling. The cluster coefficient is set to be $C = 0.15$. (a-c) R_i versus k_i for **E**, **R**, and **P** types of dynamics. (d-f) I_i versus k_i for **P**, **E**, and **R** types of dynamics. (g-i) Z_i versus k_i for **E**, **P**, and **R** types of dynamics. The scaling remains algebraic.

The resulting scaling relations are shown in Fig. 9. It can be seen that the correlation has little effect on the emergence of the three classes of algebraic scaling for the nodal resilience and influence.

4. Effect of degree heterogeneity

We generate networks with three different values of the degree heterogeneity[46–49]: $\nu = 2.1$, 3, and 4. The resulting scaling relations are shown in Fig. 10. It can be seen that the degree heterogeneity has little effect on the algebraic scaling for the nodal resilience and influence.

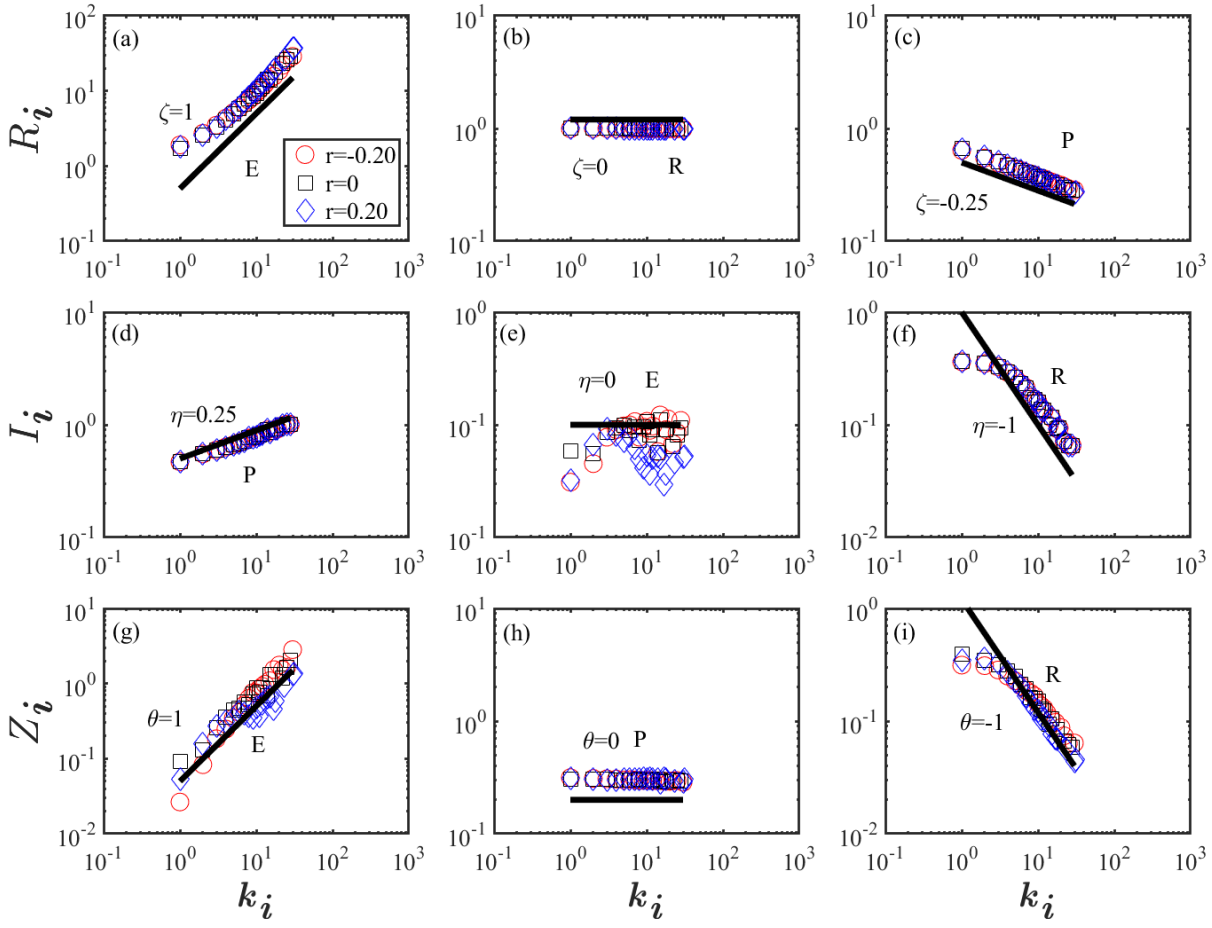

FIG. 9. Impact of degree-degree correlation on nodal resilience and influence scaling. Three values of the correlation are used: $r = -0.2$, 0, and 0.2. (a-c) R_i versus k_i for **E**, **R**, and **P** types of dynamics. (d-f) I_i versus k_i for **P**, **E**, and **R** types of dynamics. (g-i) Z_i versus k_i for **E**, **P** and **R** types of dynamics. The scaling remains algebraic.

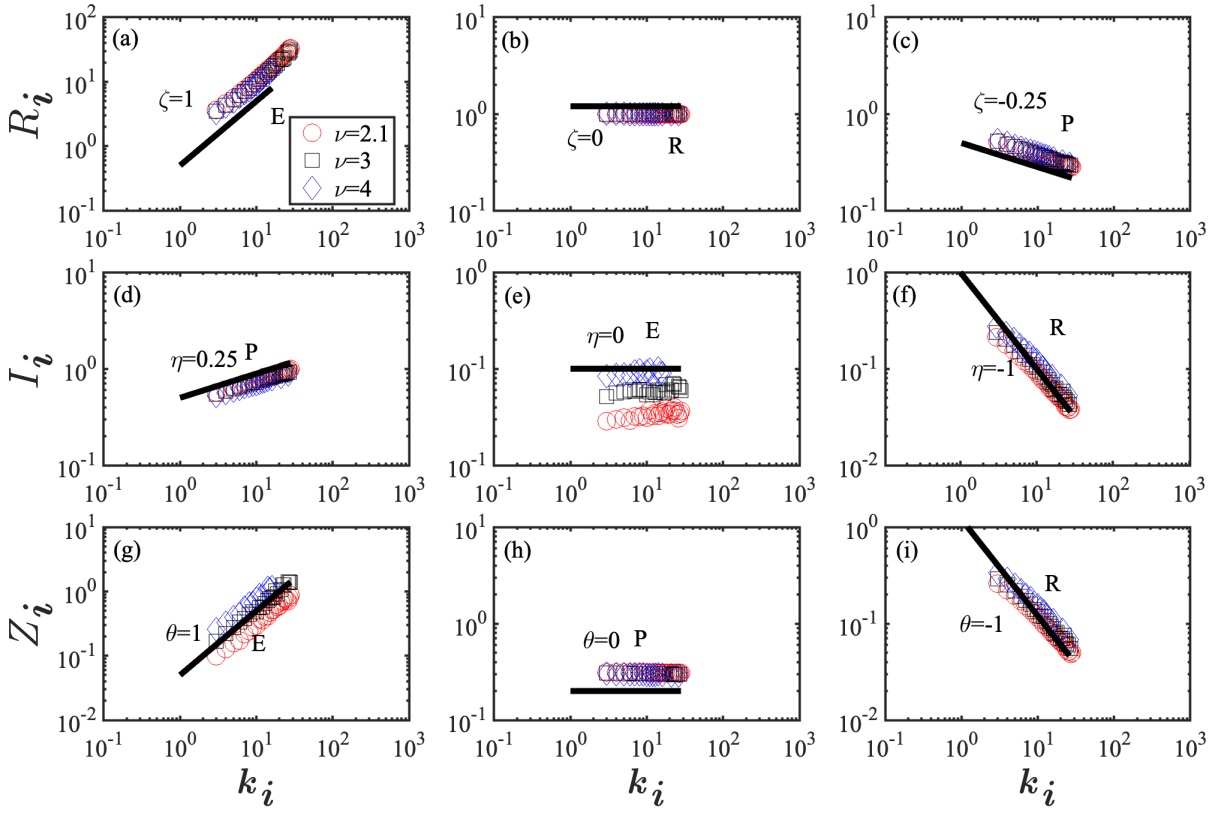

FIG. 10. Impact of degree heterogeneity on nodal resilience and influence scaling. Three values of the heterogeneity are used: $\nu = 2.1$, 3, and 4. (a-c) R_i versus k_i for **E**, **R**, and **P** types of dynamics. (d-f) I_i versus k_i for **P**, **E**, and **R** types of dynamics. (g-i) Z_i versus k_i for **E**, **P** and **R** types of dynamics. The scaling remains to be algebraic.

[1] P. Erdös and A. Rényi, "On random graphs I," Publ. Math. Debrecen **6**, 290–291 (1959).
[2] D. J. Watts and S. H. Strogatz, "Collective dynamics of 'small-world'networks," Nature **393**, 440–442 (1998).
[3] A.-L. Barabási and R. Albert, "Emergence of scaling in random networks," Science **286**, 509–512 (1999).
[4] R. Albert and A.-L. Barabási, "Statistical mechanics of complex networks," Rev. Mod. Phys. **74**, 47 (2002).
[5] C. Song, S. Havlin, and H. A. Makse, "Self-similarity of complex networks," Nature **433**, 392–395 (2005).
[6] R. Pastor-Satorras and A. Vespignani, "Epidemic spreading in scale-free networks," Phys. Rev. Lett. **86**, 3200 (2001).
[7] P. S. Dodds and D. J. Watts, "A generalized model of social and biological contagion," J. Theo. Biol. **232**, 587–604 (2005).
[8] R. Pastor-Satorras, C. Castellano, P. Van Mieghem, and A. Vespignani, "Epidemic processes in complex networks," Rev. Mod. Phys. **87**, 925 (2015).
[9] L. Han, Z. Lin, M. Tang, Y. Liu, and S. Guan, "Impact of human contact patterns on epidemic spreading in time-varying networks," Phys. Rev. E **107**, 024312 (2023).
[10] L. Zhao, Y.-C. Lai, K. Park, and N. Ye, "Onset of traffic congestion in complex networks," Phys. Rev. E **71**, 026125 (2005).
[11] I. Volkov, J. R. Banavar, S. P. Hubbell, and A. Maritan, "Neutral theory and relative species abundance in ecology," Nature **424**, 1035–1037 (2003).
[12] M. Pascual and J. A. Dunne, *Ecological Networks: Linking Structure to Dynamics in Food Webs* (Oxford University Press, 2006).
[13] J. Jiang, Z.-G. Huang, T. P. Seager, W. Lin, C. Grebogi, A. Hastings, and Y.-C. Lai, "Predicting tipping points in mutualistic networks through dimension reduction," Proc. Nat. Acad. Sci. (USA) **115**, E639–E647 (2018).
[14] A. E. Motter and Y.-C. Lai, "Cascade-based attacks on complex networks," Phys. Rev. E **66**, 065102(R) (2002).
[15] L. Zhao, K. Park, and Y.-C. Lai, "Attack vulnerability of scale-free networks due to cascading breakdown," Phys. Rev. E **70**, 035101(R) (2004).
[16] L. Zhao, K. Park, Y.-C. Lai, and N. Ye, "Tolerance of scale-free networks against attack-induced cascades," Phys. Rev. E **72**, 025104(R) (2005).
[17] S. Balaji, M. M. Babu, L. M. Iyer, N. M. Luscombe, and L. Aravind, "Comprehensive analysis of combinatorial regulation using the transcriptional regulatory network of yeast," J. Mole. Biol. **360**, 213–227 (2006).
[18] S. Maslov and I. Ispolatov, "Propagation of large concentration changes in reversible protein-binding networks," Proc. Nat. Acad. Sci. (USA) **104**, 13655–13660 (2007).
[19] G. Karlebach and R. Shamir, "Modelling and analysis of gene regulatory networks," Nat. Rev. Mole. Cell Biol. **9**, 770–780 (2008).
[20] S. Bornholdt, "Boolean network models of cellular regulation: prospects and limitations," J. R. Soc Interface **5**, S85–S94 (2008).
[21] A. Kumar, S. Rotter, and A. Aertsen, "Spiking activity propagation in neuronal networks: reconciling different perspectives on neural coding," Nat. Rev. Neurosci. **11**, 615–627 (2010).
[22] C. Li and J. Wang, "Landscape and flux reveal a new global view and physical quantification of mammalian cell cycle," Proc. Nat. Acad. Sci. (USA) **111**, 14130–14135 (2014).
[23] D. A. Rand, A. Raju, M. Sáez, F. Corson, and E. D. Siggia, "Geometry of gene regulatory dynamics," Proc. Nat. Acad. Sci. (USA) **118**, e2109729118 (2021).
[24] W.-X. Wang, L. Huang, and Y.-C. Lai, "Universal dynamics on complex networks," Europhys. Lett. (EPL) **87**, 18006 (2009).
[25] B. Barzel and A.-L. Barabási, "Universality in network dynamics," Nat. Phys. **9**, 673–681 (2013).
[26] J. Gao, B. Barzel, and A.-L. Barabási, "Universal resilience patterns in complex networks," Nature **530**, 307–312 (2016).
[27] U. Harush and B. Barzel, "Dynamic patterns of information flow in complex networks," Nat. Commun. **8**, 2181 (2017).
[28] C. Hens, U. Harush, S. Haber, R. Cohen, and B. Barzel, "Spatiotemporal signal propagation in complex networks," Nat. Phys. **15**, 403–412 (2019).
[29] C. Meena, C. Hens, S. Acharyya, S. Haber, S. Boccaletti, and B. Barzel, "Emergent stability in complex network dynamics," Nat. Phys. **19**, 1033–1042 (2023).
[30] G. Moutsinas and W. Guo, "Node-level resilience loss in dynamic complex networks," Sci. Rep. **10**, 3599 (2020).
[31] M. Kitsak, L. K. Gallos, S. Havlin, F. Liljeros, L. Muchnik, H. E. Stanley, and H. A. Makse, "Identification of influential spreaders in complex networks," Nat. Phys. **6**, 888–893 (2010).
[32] X. Liu, D. Li, M. Ma, B. K. Szymanski, H. E. Stanley, and J. Gao, "Network resilience," Phys. Rep. **971**, 1–108 (2022).
[33] J. Gao, X. Liu, D. Li, and S. Havlin, "Recent progress on the resilience of complex networks," Energies **8**, 12187–12210 (2015).
[34] C. Zhang, X. Xu, and H. Dui, "Resilience measure of network systems by node and edge indicators," Reli. Eng. Sys. Safety **202**, 107035 (2020).
[35] X. Wu, L. Fu, Z. Zhang, H. Long, J. Meng, X. Wang, and G. Chen, "Evolving influence maximization in evolving networks," ACM Trans. Internet Tech. **20**, 1–31 (2020).
[36] A. Ullah, B. Wang, J. Sheng, J. Long, N. Khan, and Z. Sun, "Identification of nodes influence based on global structure model in complex networks," Sci. Rep. **11**, 6173 (2021).
[37] A. S. Novozhilov, G. P. Karev, and E. V. Koonin, "Biological applications of the theory of birth-and-death processes," Brief. Bioinform. **7**, 70–85 (2006).
[38] M. Bruneau, S. E. Chang, R. T. Eguchi, G. C. Lee, T. D. O'Rourke, A. M. Reinhorn, M. Shinozuka, K. Tierney, W. A. Wallace, and D. Von Winterfeldt, "A framework to quantitatively assess and enhance the seismic resilience of communities," Earthq. Spec. **19**, 733–752 (2003).
[39] H. Yu, P. Braun, M. A. Yıldırım, I. Lemmens, K. Venkatesan, J. Sahalie, T. Hirozane-Kishikawa, F. Gebreab, N. Li, N. Simonis, *et al.*, "High-quality binary protein interaction map of the yeast interactome network," Science **322**, 104–110 (2008).
[40] J.-F. Rual, K. Venkatesan, T. Hao, T. Hirozane-Kishikawa, A. Dricot, N. Li, G. F. Berriz, F. D. Gibbons, M. Dreze, N. Ayivi-Guedehoussou, *et al.*, "Towards a proteome-scale map of the human protein–protein interaction network," Nature **437**, 1173–1178 (2005).
[41] K. Ikehara and A. Clauset, "Characterizing the structural diversity of complex networks across domains," arXiv preprint arXiv:1710.11304 (2017).
[42] M. De Domenico, V. Nicosia, A. Arenas, and V. Latora, "Structural reducibility of multilayer networks," Nat. Commun. **6**, 6864 (2015).
[43] "U. rovira i virgili network dataset – KONECT," (2017).
[44] T. Opsahl and P. Panzarasa, "Clustering in weighted networks," Soc. Net. **31**, 155–163 (2009).
[45] Q. Su, L. Aming, W. Long, and E. H. Stanley, "Spatial reciprocity in the evolution of cooperation," R. Soc. B. **286**, 20190041 (2019).
[46] P. L. Krapivsky, S. Redner, and F. Leyvraz, "Connectivity of growing random networks," Phys. Rev. Lett. **85**, 4629–4632 (2000).
[47] K.-I. Goh, B. Kahng, and D. Kim, "Universal behavior of load distribution in scale-free networks," Phys. Rev. Lett. **87**, 278701 (2001).
[48] Q. Su, A. McAvoy, Y. Mori, and J. B. Plotkin, "Evolution of prosocial behaviours in multilayer populations," Nat. Human. Behav. **6**, 338–348 (2022).
[49] Q. Su, B. Allen, and J. B. Plotkin, "Evolution of cooperation with asymmetric social interactions," Proc. Nat. Acad. Sci. (USA) **119**, e2113468118 (2021).